Experimentally determined oscillator strengths in Rh II

2013 J. Phys. B: At. Mol. Opt. Phys. 46 205001

(http://iopscience.iop.org/0953-4075/46/20/205001)

OPEN ACCESS
IOP PUBLISHING
JOURNAL OF PHYSICS B: ATOMIC, MOLECULAR AND OPTICAL PHYSICS
J. Phys. B: At. Mol. Opt. Phys. **46** (2013) 205001 (6pp)
doi:10.1088/0953-4075/46/20/205001

Experimentally determined oscillator strengths in Rh II

E Bäckström[1], H Nilsson[2], L Engström[3], H Hartman[2,4] and S Mannervik[1]

[1] Department of Physics, Stockholm University, AlbaNova University Center, SE-1069 Stockholm, Sweden
[2] Lund Observatory, Box 43, SE-22100 Lund, Sweden
[3] Department of Physics, Lund University, Box 118, SE-22100 Lund, Sweden
[4] Material Sciences and Applied Mathematics, Faculty of Technology, Malmö University, SE-20506 Malmö, Sweden

E-mail: erik.backstrom@fysik.su.se

Received 23 June 2013, in final form 20 August 2013
Published 26 September 2013
Online at stacks.iop.org/JPhysB/46/205001

Abstract
This paper presents new experimentally determined branching fractions and oscillator strengths (log gf) for lines originating from 17 levels belonging to 5 terms of the first excited odd configuration $4d^7(^4D)5p$ in Rh II. The intensity calibrated spectra of Rh II have been recorded with a Fourier transform spectrometer between 25000 and 45000 cm^{-1} (2200–4000 Å). In this region, 49 lines have been identified and measured. By combining the branching fractions obtained from the spectra with previously measured lifetimes, log gf values are reported. The new results are compared with previous theoretical work.

(Some figures may appear in colour only in the online journal)

1. Introduction

Rhodium is one of the most expensive metals on earth and finds its use in the automotive industry as a catalyst. Of more scientific interest is the fact that rhodium has been detected in the spectra of many astrophysical objects e.g. the sun [1], and the HgMn-type stars χ Lupi [2], HD 65949 [3] and HD 175640 [4]. The need for accurate and reliable atomic data in order to investigate high-resolution spectra from objects such as these is significant, and to the best of our knowledge no experimental oscillator strengths are available for Rh II. In a recently published study, Quinet *et al* [5] combined measured lifetimes with theoretical branching fractions (BFs) and derived semi-empirical oscillator strengths. The lifetime measurements were performed on ions in a laser-generated plasma employing the time-resolved laser-induced-fluorescence technique, and the calculations were performed with a relativistic Hartree–Fock model with core-polarization (HFR+CPOL). This paper aims to experimentally evaluate the reliability of these oscillator strengths and further enhance our knowledge of Rh II.

A schematic drawing of the lower part of the energy level structure of singly charged rhodium can be seen in figure 1. When measuring BFs, extensive knowledge of the energy level structure of the system of interest is necessary since accurate values require the measurements of all lines originating from an upper level. The line list used in this work was compiled by Kramida *et al* [6] and based on earlier work by Sancho [7]. In this study, BFs for transitions from terms belonging to the first excited $d^7(^4D)5p$ configuration are measured and combined with previously published experimental lifetimes [5]. More specifically, levels belonging to the terms z^5F^o, z^5D^o, z^5G^o, z^3F^o and z^3G^o are investigated.

The main decay channel for the quintet terms in the $4d^7(^4D)5p$ configuration is to levels in the a^5F term belonging to the configuration $4d^7(^4F)5s$. However, they also decay by inter-combination transitions to states in the ground configuration ($4d^8$ a^3F). The latter transitions fall in the vacuum UV, and cannot be measured in the present experiment. This is a potential problem in the BF determinations for these levels. However, in most cases, the inter-combination lines

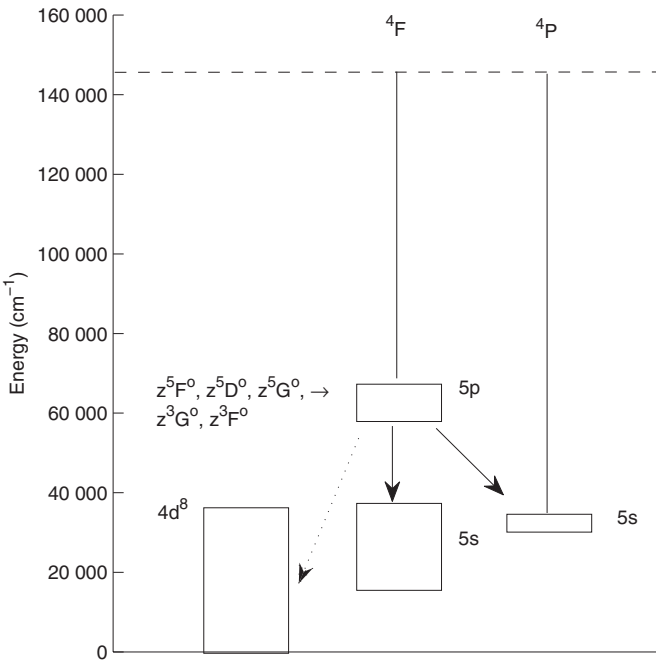

Figure 1. An energy level diagram of singly ionized rhodium. The solid arrows show transitions that can be readily measured with our experimental setup. The dashed line indicates transitions down to the ground configuration which, in some cases, fall outside the range of our setup.

are weak and their influence can be estimated from these theoretical calculations.

2. Experiment

To determine the oscillator strengths, it is necessary to measure the lifetime of the upper level as well as the relative intensities of all lines originating from that level. The branching fraction, BF, is defined as

$$\mathrm{BF}_{ul} = A_{ul} \Big/ \sum_k A_{uk} = I_{ul} \Big/ \sum_k I_{uk}, \qquad (1)$$

where u labels the upper and l the lower level, respectively. A is the transition probability and I is the measured intensity in units of number of photons per second on an accurately calibrated scale over the whole wavelength range. Combining the BFs with the lifetime defined as

$$\tau_u = 1 \Big/ \sum_k A_{uk} \qquad (2)$$

allows for the extraction of the individual A_{ul}-values as

$$A_{ul} = \mathrm{BF}_{ul}/\tau_u. \qquad (3)$$

The oscillator strength, f_{lu}, is then derived through the formula

$$f_{lu} = 1.499 \times 10^{-16} \times \frac{g_u \lambda_{ul}^2}{g_l} A_{ul}, \qquad (4)$$

where g is the statistical weight and λ_{ul} is the wavelength (in Å) of the transition in question.

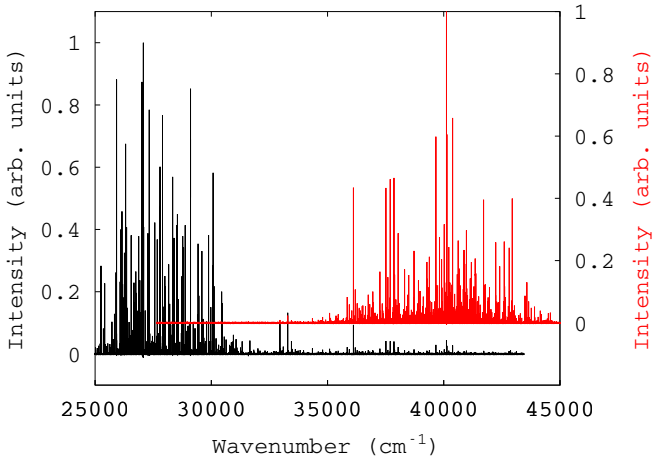

Figure 2. Two spectra recorded with different detectors, Hamamatsu 1P28 (below) and Hamamatsu R166 (above). The intensity scales are shifted vertically for the purpose of illustration. Lines in the overlapping region are used to relate the different intensity scales.

2.1. Determination of branching fractions

A hollow cathode (HC) discharge was used as the emission light source. The HC has a hollow iron core where a thin foil, 0.125 mm thick and 25 × 25 mm wide, was inserted. The foil consisted of 99.9% rhodium. The HC was operated at currents between 0.1 and 1 A and neon was used as a carrier gas. The typical pressures during the measurements were around 1.6–1.8 torr. The light emitted from the cathode was analysed by an FTS instrument (Chelsea Instruments FT500).

The instrument itself restricts the wavelength region to be covered in the spectra since it has a beamsplitter which cuts off at 1850 Å. However, this was not the main limitation since the optical path between the HC and the FTS instrument was in air, hence no wavelengths below 2000 Å could be measured. Another restriction posed on the obtained spectra is the sensitivity of the detectors used when recording the spectra. To cover the region of interest, two different detectors were used. In the region between 25000 and 40000 cm^{-1}, a Hamamatsu 1P28 photo multiplier tube (PMT) was used, whereas the region between 35000 and 45000 cm^{-1} was covered by a Hamamatsu R166 PMT. To avoid the aliasing inherent in the FTS method, a standard UG5 coloured glass filter (cutoff around 6500 Å) was used in combination with the 1P28 detector to limit the aliasing with longer wavelengths where the detector is sensitive. In figure 2, two complete spectra recorded with the two different detector setups are shown, displaying their sensitivity, as well as their relative strengths in the overlapping region.

Promptly after measuring a series of rhodium spectra, a spectrum of a calibrated deuterium lamp was recorded. The deuterium spectrum was then used to determine the response of the detectors. For the determination of BFs, no absolute calibration is necessary; only the relative intensities are of interest. However, the spectra recorded with the different detectors have to be brought to a common scale. This was done by comparing the intensities of lines recorded by both detectors in the overlapping region. Thus, the scaling factor between the two regions was determined by taking the ratios

Table 1. Experimental oscillator strengths, log gf values and branching fractions together with theoretical.

				BF			log gf	
Upper level	τ[a] (ns)	Lower level	λ[b] (nm)	Theory[a]	Exp.	Uncertainty (%)	log(gf)	Uncertainty (%)
$z^5G^o_6$	3.0(2)	$z^5G^o_6$	233.477	1	1	0	0.549	6.7
$z^5F^o_4$	3.9(5)	a^5F_5	252.052	0.874	0.874	0.8	0.284	12.8
		a^5F_4	263.033	0.068	0.078	7.1	−0.730	14.7
		b^3F_4	320.725	0.022	0.017	6.8	−1.22	14.5
		a^5P_3	347.776*	0.019	0.014	6.7	−1.24	14.5
		Residual		0.017				
$z^5F^o_5$	3.8(3)	a^5F_5	249.079	0.957	0.969	0.2	0.416	7.9
		b^3F_4	315.929	0.038	0.027	7.0	−0.932	10.6
		Residual		0.004				
$z^5F^o_3$	3.8(3)	a^5F_4	251.065	0.878	0.875	1.0	0.183	8.0
		a^5F_3	259.216	0.076	0.087	9.6	−0.792	12.4
		b^3F_3	323.332	0.020	0.015	7.9	−1.362	11.2
		a^5P_2	330.734*	0.017	0.013	7.8	−1.395	11.1
		residual		0.009				
$z^5D^o_4$	3.3(2)	a^5F_5	236.467	0.051	0.069	7.0	−0.801	9.3
		a^5F_4	246.103	0.912	0.901	0.7	0.348	6.1
		a^5P_3	318.783	0.033	0.026	7.2	−0.972	9.4
		Residual		0.004				
$z^5F^o_2$	3.8(3)	a^5F_3	250.512	0.826	0.821	1.5	7.24×10^{-3}	8.0
		a^5F_2	255.992	0.120	0.126	9.1	−0.789	12.0
		Residual		0.038				
$z^5G^o_5$	3.5(2)	a^5F_5	233.330	0.066	0.074	18.3	−0.719	19.2
		a^5F_4	242.709	0.568	0.625	2.8	0.239	6.4
		b^3F_4	291.015	0.313	0.247	5.3	-5.84×10^{-3}	7.8
		Residual		0.053				
$z^5D^o_3$	3.4(4)	a^5F_4	238.545	0.047	0.058	7.8	−0.99	14.0
		a^5F_3	245.890	0.891	0.883	0.7	0.22	11.8
		a^5P_2	309.344	0.028	0.025	8.8	−1.14	14.7
		Residual		0.034				
$z^5G^o_4$	3.3(3)	a^5F_3	241,584	0.708	0.746	1.6	0.25	8.2
		b^3F_4	279.278	0.036	0.027	19.7	−1.06	21.3
		b^3F_3	296.354	0.115	0.086	6.7	−0.51	10.5
		Residual		0.140				
$z^5D^o_2$	3.7(5)	a^5F_3	240.522	0.088	0.090	7.0	−0.98	15.2
		a^5F_2	245.571	0.809	0.819	1.1	-2.60×10^{-5}	13.6
		a^5P_2	300.898	0.049	0.040	8.8	−1.13	16.1
		a^5P_1	309.675	0.021	0.020	11.5	−1.41	17.8
		Residual		0.031				
$z^5G^o_3$	3.3(2)	a^5F_2	242.100	0.832	0.859	1.0	0.204	6.3
		b^3F_3	289.763	0.019	0.016	29.8	−1.36	30.4
		b^3F_2	301.978	0.057	0.033	10.0	−1.02	11.8
		Residual		0.093				
$z^3G^o_5$	3.2(2)	a^5F_4	229.004	0.587	0.577	2.8	0.193	6.9
		b^3F_4	271.527	0.352	0.361	4.3	0.137	7.6
		Residual		0.062				
$z^5G^o_2$	3.3(3)	a^5F_1	243.185	0.875	0.897	0.9	0.081	9.1
		b^3F_2	298.830	0.049	0.027	19.1	−1.27	21.1
		Residual		0.076				
$z^3G^o_4$	3.4(2)	a^5F_3	226.343	0.313	0.300	4.5	−0.214	7.4
		b^3F_3	273.740	0.464	0.476	3.1	0.151	6.7
		a^5P_3	276.483	0.087	0.088	7.2	−0.575	9.3
		Residual		0.136				
$z^3F^o_4$	2.4(2)	a^5F_3	235.035	0.045	0.049	7.0	−0.817	9.2
		b^3F_4	270.560	0.477	0.473	2.7	0.289	6.5
		Residual		0.478				
$z^3F^o_3$	2.3(3)	a^5F_2	233.530	0.042	0.030	14.4	−1.13	19.4
		b^3F_4	262.541	0.360	0.394	3.6	0.093	13.5
		b^3F_3	277.577	0.098	0.075	10.0	−0.577	16.4
		residual		0.501				

Table 1. (Continued.)

				BF			log gf	
Upper level	τ[a] (ns)	Lower level	λ[b] (nm)	Theory[a]	Exp.	Uncertainty (%)	log(gf)	Uncertainty (%)
$z^3G^o_3$	2.0(3)	a^5F_2	223.771	0.099	0.095	8.8	−0.602	17.4
		b^3F_4	250.276	0.088	0.082	5.9	−0.566	16.1
		b^3F_3	263.900	0.078	0.076	6.4	−0.554	16.1
		a^5P_3	266.448	0.022	0.021	17.9	−1.11	23.4
		b^3F_2	273.992	0.229	0.241	4.1	−0.022	15.6
		Residual		0.483				

[a] Lifetimes and theoretical BFs from Quinet *et al* [5].

[b] The wavelengths are from Sancho [7] except the starred ones which are calculated from the energy levels.

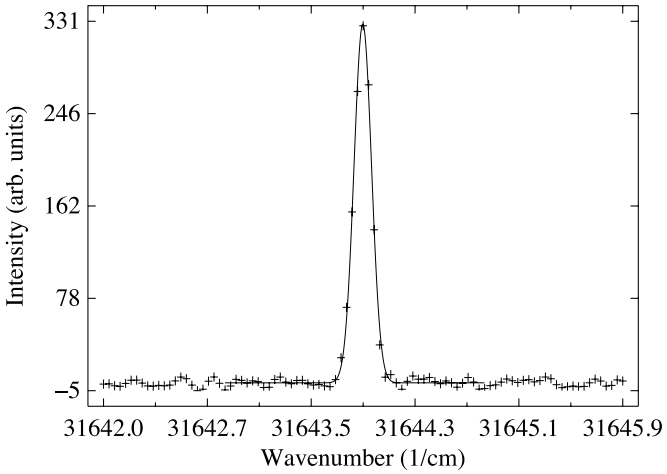

Figure 3. The observed line corresponding to the b^3F_4—$z^5F^o_5$ transition around 31 643.9 cm^{-1} together with a fitted Gaussian line shape function.

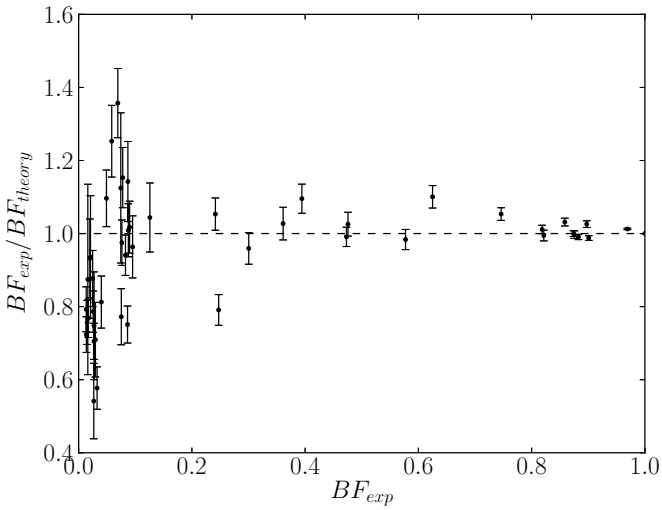

Figure 4. Ratio between our measured branching fractions, BF_{exp}, and the theoretical branching fractions from [5], BF_{theory}, plotted against BF_{exp}.

between a number of lines recorded by both detectors. The variation of this ratio gives an uncertainty in the detector response determination. The wavenumber scale is given by an internal laser in the FTS controlling the sampling rate. The relative uncertainty in the wavenumber scale is around 10^{-6} and allowed us to unambiguously identify all the lines of interest.

3. Results

Rhodium has only one stable isotope which makes the interpretation of the spectra easier with no isotope shift present. Furthermore, it has a nuclear spin of $I = 1/2$ so at most two possible hyperfine components of each level are possible. However, this splitting was too small to be resolved. For all the observed lines, the GFit [8] software was used to fit Gaussian line shapes to determine line positions as well as to obtain the area of the peaks.

The fits were in general good and the result of one particular fit can be seen in figure 3. The line in the figure has a full-width at half-maximum of 0.155(2) cm^{-1} at 31643.9 cm^{-1}. For some of the strongest lines (with A-values around 10^9 s^{-1}), a small asymmetry was observed which affected the goodness-of-fit, but to a lesser extent the uncertainty in the area determination. The reason for this asymmetry is most likely imperfections in the alignment of the optical path of the FTS instrument. In the determination of the oscillator strengths, there are several uncertainties contributing to the final uncertainty stated in table 1: the uncertainty in the area determination, the intensity calibration of the spectra (with the use of the deuterium lamp) and the lifetime. These are then added quadratically to obtain the total uncertainty. A detailed description of the uncertainty analysis can be found in [9]. In general, the main contributor to the uncertainty budget is the previously measured lifetimes, which in some cases have uncertainties around 15%.

Whether a line is observed or not is due to the combination of the sensitivity of the detection setup at the wavelength of the line and the intrinsic line strength. In general, lines weaker than $A \approx 4 \times 10^7$ s^{-1} [5] were not observed or the signal-to-noise ratio was too low to provide a satisfactory fit of the observed line. Contributions from lines not measurable in the spectra or outside of the range of the detectors are summed up using the theoretical BF from Quinet *et al* [5] into a residual. The experimental BFs are then adjusted to accommodate the missing branches, i.e. they are scaled down to make the sum of all measured- and estimated-residual branches equal to 1. The main decay channel for some of the triplet terms is to the ground configuration. The estimation of the missing branches for these levels can therefore be up to around 50%.

The result can be seen in table 1. The log(gf) values ordered by wavelength can also be found in table 2. The

Table 2. A findings list with experimental log gf ordered by increasing wavelength.

λ[a] (nm)	log(gf)	Uncertainty
223.771	−0.602	17.4%
226.343	−0.214	7.4%
229.004	0.193	6.9%
233.330	−0.719	19.1%
233.477	0.549	12.8%
233.530	−1.13	19.4%
235.035	−0.817	9.2%
236.467	−0.801	9.2%
238.545	−0.989	14.1%
240.522	−0.977	15.2%
241.584	−0.25	8.3%
242.100	0.204	6.3%
242.709	0.239	6.4%
243.185	0.0811	9.1%
245.571	-2.62×10^{-5}	13.6%
245.890	0.217	11.8%
246.103	0.348	6.1%
249.079	0.416	7.9%
250.276	−0.566	16.1%
250.512	0.00724	8.0%
251.065	0.183	8.0%
252.052	0.284	12.8%
255.992	−0.789	12.0%
259.216	−0.792	12.4%
262.541	0.0933	13.5%
263.033	−0.73	14.7%
263.900	−0.554	16.3%
266.448	−1.11	23.4%
270.560	0.289	6.5%
271.527	0.137	7.6%
273.740	0.151	6.7%
273.992	−0.0217	15.6%
276.483	−0.575	9.3%
277.577	−0.577	16.4%
279.278	−1.06	21.3%
289.763	−1.36	30.4%
291.015	−0.00584	7.8%
296.354	−0.509	10.5%
298.830	−1.27	21.1%
300.898	−1.13	16.1%
301.978	−1.02	11.8%
309.344	−1.14	14.7%
309.675	−1.41	17.8%
315.926	−0.932	10.6%
318.783	−0.972	9.4%
320.725	−1.22	14.5%
323.332	−1.36	11.2%
330.734*	−1.39	11.1%
347.776*	−1.24	14.5%

[a] The wavelengths are from Sancho except the starred which are calculated from the energy levels.

agreement between the theoretical and experimental BFs is in general good. The ratio between the experimental and theoretical BFs plotted against the experimental BFs can be seen in figure 4 and against the wavenumbers in figure 5. In figure 4, it can be seen that the weaker lines have larger uncertainties, originating primarily from the uncertainty in the area determination of the peaks. It can also be seen that the ratios form two groups, one which is centred slightly above and the other slightly below. When looking in more detail, it is found that spin-forbidden lines from the quintet to triplet states

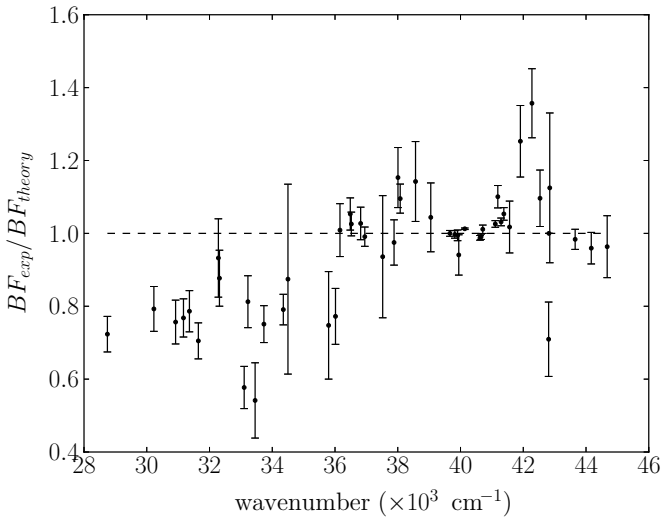

Figure 5. Ratio between our measured branching fractions, BF_{exp}, and the theoretical branching fractions from Quinet *et al* [5], BF_{theory}, plotted against wavenumber.

(e.g. b^3F_4–$z^5F^o_4$) are seen below one group and spin-allowed (e.g. a^5F_3–$z^5F^o_3$) lines are seen in the other group. This trend suggests that the mixing of levels in the calculations could be overestimated, resulting in stronger spin-forbidden lines. The same trend can be seen in figure 5 where the spin-forbidden lines, with in general lower wavenumbers due to the energy level structure, can be seen to the left in the picture and the allowed to the right, indicating as in figure 4, that the mixing is overestimated in the calculation.

4. Conclusions

Branching fractions for 49 Rh II lines were measured for the first time using an FTS instrument and an emission source. The BFs have been combined with previously measured lifetimes by Quinet *et al* [5], to yield oscillator strengths for these transitions. The deviations between our measured and the theoretical BFs are mostly within the uncertainty limits. However, our data suggest a slight overestimation of the mixing leading to higher theoretical BFs—and thus log(gf)—for the spin-forbidden lines.

Acknowledgments

This work was supported by the Swedish Research Council (VR) through grants 2008-3736 and 2006-3085. HN, LE and HH acknowledge the support of the Linneaus grant to the Lund Laser Centre from the Swedish Research Council.

References

[1] Moore C E, Minnaert M G J and Houtgast J 1966 *The Solar Spectrum 2935 Å to 8770 Å (NBS Monograph* vol 61*)* (Washington DC: US Department of Commerce)

[2] Lundberg H, Johansson S, Litzén U, Wahlgren G M and Leckrone S 1998 *The Scientific Impact of the Goddard High Resolution Spectrograph (ASP Conference Series* vol 143*)* (California, CA: Astronomical Society of the Pacific) p 343

[3] Cowley C R, Hubrig S, Palmeri P, Quinet P, Biémont É, Wahlgren G M, Schütz O and González J F 2010 *Mon. Not. R. Astron. Soc.* **405** 1271–84
[4] Castelli F and Hubrig S 2004 *Astron. Astrophys.* **425** 263–70
[5] Quinet P, Biémont É, Palmeri P, Engström L, Hartman H, Lundberg H and Nilsson H 2012 *Astron. Astrophys.* **537** A74
[6] Kramida A, Ralchenko Y, Reader J and NIST ASD Team 2012 *NIST Atomic Spectra Database (ver. 5.0)* http://physics.nist.gov/asd
[7] Sancho F J 1958 *Ann. Fis. Quim.* **54** 41–64
[8] Engström L 1998 *Lund Reports in Atomic Physics Report No. LRAP-23* (Lund: Atomic Physics, Lund University)
[9] Sikström C M, Nilsson H, Litzén U, Blom A and Lundberg H 2002 *J. Quantum. Spectrosc. Radiat. Transfer* **74** 355–68